Accepted Manuscript

Ultrasensitive electrochemical detection of *Mycobacterium tuberculosis* IS6110 fragment using gold nanoparticles decorated fullerene nanoparticles/nitrogen-doped graphene nanosheet as signal tags

Lijuan Bai, Yuhan Chen, Xinzhu Liu, Jing Zhou, Jun Cao, Liang Hou, Shuliang Guo

PII: S0003-2670(19)30768-8

DOI: https://doi.org/10.1016/j.aca.2019.06.043

Reference: ACA 236885

To appear in: *Analytica Chimica Acta*

Received Date: 5 May 2019

Revised Date: 19 June 2019

Accepted Date: 21 June 2019

Please cite this article as: L. Bai, Y. Chen, X. Liu, J. Zhou, J. Cao, L. Hou, S. Guo, Ultrasensitive electrochemical detection of *Mycobacterium tuberculosis* IS6110 fragment using gold nanoparticles decorated fullerene nanoparticles/nitrogen-doped graphene nanosheet as signal tags, *Analytica Chimica Acta*, https://doi.org/10.1016/j.aca.2019.06.043.

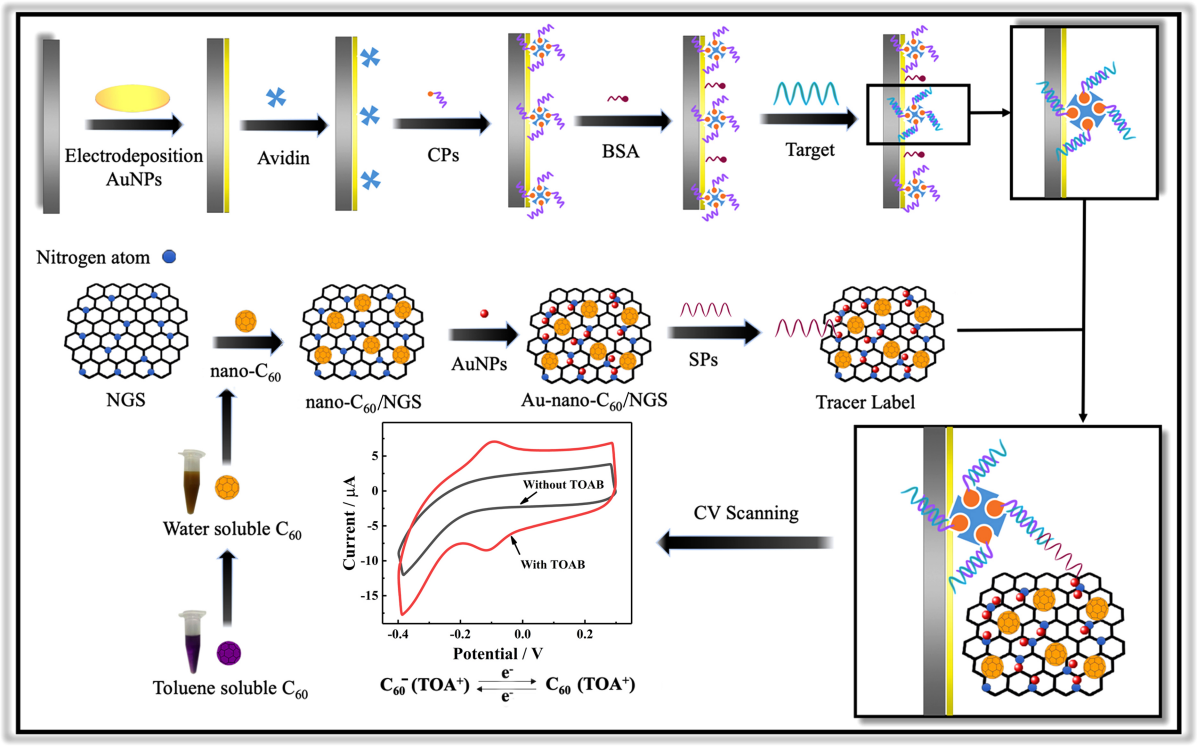

Ultrasensitive electrochemical detection of *Mycobacterium tuberculosis* IS6110 fragment using gold nanoparticles decorated fullerene nanoparticles/nitrogen-doped graphene nanosheet as signal tags

Lijuan Bai[a1], Yuhan Chen[b1], Xinzhu Liu[b], Jing Zhou[a], Jun Cao[c], Liang Hou[a], Shuliang Guo[b]

[a] *Engineering Technology Research Center for Pharmacodynamic Evaluation of Chongqing, College of Pharmacy, Chongqing Medical University, Chongqing 400016, PR China*

[b] *Department of Respiratory and Critical Care Medicine, the First Affiliated Hospital of Chongqing Medical University, Chongqing 400016, PR China*

[c] *Department of Respiratory and Critical Care Medicine, West China Hospital of Sichuan University, Chengdu 610041, PR China*

Abstract: Tuberculosis (TB), caused by *Mycobacterium tuberculosis* (MTB), remains the top fatal infection continuing to threat public health, and the present detection method for MTB is facing great challenges with the global TB burden. In response to this issue, a novel electrochemical DNA biosensor was developed for detecting the IS6110 fragment within MTB. For the first time, the nanohybrid of gold nanoparticles decorated fullerene nanoparticles/nitrogen-doped graphene nanosheet (Au-nano-C_{60}/NGS) directly served as a new signal tag to generate signal response without additional redox molecules and subsequently labeled with signal probes (SPs) to form tracer label to achieve signal amplification. Additionally, a biotin-avidin system was introduced to immobilize abundant capture probes (CPs), further improving the sensitivity of the proposed biosensor. After a

* Corresponding author. Tel: +86-023-89012097; Fax: +86-023-89012833. *E-mail address*: guosl999@sina.com (S. Guo)

[1] These two authors contributed equally to this work.

typical sandwich hybridization, the proposed electrochemical DNA biosensor was incubated with tetraoctylammonium bromide (TOAB), which was used as a booster to induce the intrinsic redox activity of the tracer label, resulting in a discriminating current response. The proposed electrochemical DNA biosensor shows a broad linear range for MTB determination from 10 fM to 10 nM with a low limit of detection (LOD) of 3 fM. In addition, this proposed biosensor not only distinguishes mismatched DNA sequence, but also differentiates MTB from other pathogenic agents. More importantly, it has been preliminarily applied in clinical detection and displayed excellent ability to identify the PCR products of clinical samples. There is great potential for this developed method to be used in early diagnosis and monitor of TB.

Keywords: C_{60}-based signal tag; sandwich-type assay; biotin-avidin system; TB diagnosis

1. Introduction

Tuberculosis (TB) is among the top ten causes of death around the world and a profound burden on public health. Vast gaps in detection and treatment of TB persistently exist, which are in part attributed to misdiagnosis. A definite diagnosis of TB relies on detection of the infectious agent, mainly *Mycobacterium tuberculosis* (MTB) with culture and microscopy, which are limited by low detection rate and long duration [1]. Meanwhile, novel approaches, in particular genetic and molecular techniques, are being developed for fast detection of MTB [2]. IS6110, an insertion element which is unique to MTB and differs in repeat counts in each strain of the MTB complex, stands out as a diagnosis marker and a tool in molecular epidemiology [3, 4]. It is therefore utilized as a target marker for MTB detection in this work.

Electrochemical DNA biosensors, a novel analytical tool, have attracted considerable

attention in pathogen detection due to simple operational procedures, low cost, as well as high sensitivity and stability [5-7]. To assist the diagnosis of MTB with IS6110, it is crucial to develop a highly sensitive electrochemical biosensor for DNA detection. It has been proved that nanomaterials both as redox probes and nanocarriers can effectively enhance the sensitivity of the biosensors because of the advantages of sufficient active binding sites, outstanding electrocatalytic activities and stable signal responses [8-10]. Fullerene (C_{60}) possesses outstanding inherent redox activity absent in other carbon materials and holds great potential for development of highly sensitive biosensors [11-14]. However, the sole use of C_{60} cannot achieve effective signal amplification [15]. Fortunately, modification of C_{60} with other substances could enhance its analytical performance, which provides a novel insight in C_{60}-based biosensor development [16-18].

Recently, nitrogen-doped graphene nanosheet (NGS) has aroused great interest in many aspects such as supercapacitors [19], electrocatalyst [20] and sensing [21] due to its excellent electrical conductivity, electrocatalytic property and electron density caused by incorporation of nitrogen. More importantly, nitrogen-doped graphene is a potential support matrix with a unique enhancement effect when combined with various materials, such as TiO_2 [22], Fe_3O_4 [23], MoS_2 [24] and so on, compared with individual component. Moreover, the rich nitrogen atoms of NGS provides abundant anchor sites for metal nanoparticles to improve their analytical performance [25], as in the NGS/gold nanoparticles (AuNPs) nanohybrid recently reported to immobilize DNA probes resulting in improved sensitivity, which offers a favorable tool for gene analysis and related disease diagnosis [26]. Inspired by these, we believed that NGS could be an ideal matrix to simultaneously load fullerene nanoparticles

(nano-C_{60}) and AuNPs to serve as an efficient and new signal tag to generate and amplify signal response and subsequently applied for MTB DNA determination.

In this work, a sandwich-type electrochemical assay for IS6110 fragment detection was successfully constructed. In order to increase the amount of capture probes (CPs) modified onto the electrode surface, the biotin-avidin system was introduced into the electrochemical assay because each avidin molecular conjugates with four biotin molecules [27-29]. Notably, the design of AuNPs decorated nano-C_{60}/NGS was presented as a new signal tag for signal generation for the first time. Incorporating NGS with nano-C_{60} resulted in high ratio surface, great conductivity, rich nitrogen atoms and outstanding redox activity. The abundant nitrogen atoms of the nano-C_{60}/NGS nanohybrid permits immobilization of plentiful AuNPs on the surface, which not only enabled labeling with abundant signal probes (SPs) via the strong Au-S bonds to form the tracer label, but also enhanced electron transfer. After the sandwich-type hybridization, the proposed electrochemical DNA biosensor was treated with tetraoctylammonium bromide (TOAB) to induce the inherent electroactivity of the tracer label, resulting in an excellent current response and a sensitive and quantitative assay for the IS6110 fragment. The analytical performance of the proposed electrochemical biosensor was compared with previously reported electrochemical biosensor for MTB detection (Table 1), and our work showed a lower detection limit and wider linear range, suggesting the proposed biosensor may be of use in the field of TB diagnosis. Fig. 1 depicted the stepwise process for the proposed electrochemical DNA biosensor construction.

2. Experimental

2.1. Reagents and Apparatus

Chlorauric acid ($HAuCl_4$) was purchased from Sigma-Aldrich Chemical Co. (USA). Nitrogen-doped graphene (NGS) and fullerene (C_{60}, 99.5%) were provided by XFNANO Nanotechnology Co., Ltd (Nanjing, China). The bacterial DNA extraction kit was purchased from Tiangen Biochemical Technology Co., Ltd (Beijing, China). Tetraoctylammonium bromide (TOAB) was provided by Yuanye Bio-Technology Co., Ltd (Shanghai, China). Specimens of sputum were collected from Department of Respiratory and Critical Care Medicine, the First Affiliated Hospital of Chongqing Medical University. $K_3Fe(CN)_6/K_4Fe(CN)_6$ solution (5 mM) containing 0.1 M KCl was used to monitor the construction of the proposed biosensor. Working buffer was phosphate buffer (PB, 0.1 M, pH 7.0) containing 2 mM $MgCl_2$ and 10 mM KCl. All other reagents were of analytical grade. The PCR primers and corresponding PCR amplification procedures were designed according to previous literatures [34-36]. All the nucleic acid used in our experiment was sythesized by Sangon Biotech. Co. Details of the oligonucleotide sequences are shown in Table 2.

The electrochemical experiments were carried out with an electrochemical workstation (CHI660E) with a typical three electrode system (Shanghai Chenhua Instrument Co, China). Glassy carbon electrode (GCE) of 4 mm diameter was used as working electrode, platinum wire as auxiliary electrode and saturated calomel electrode (SCE) as reference electrode. Cyclic voltammetry (CV) ranging from -0.2 to 0.6 V (vs. SCE) at a scan rate of 100 mV s^{-1} and electrochemical impedance spectroscopy (EIS) were used to monitor the stepwise biosensor construction in 5 mM $K_3Fe(CN)_6/K_4Fe(CN)_6$ (1:1) solution containing 0.1 M KCl. Differential pulse voltammetry (DPV) measurement of the proposed biosensor (-0.4 to 0.3 V) was performed in 0.1 M phosphate buffer (pH 7.0). Field emission scanning electron

microscope (Hitachi SU8010, Tokyo, Japan) was used for morphological depiction of the materials. UV-vis absorption was obtained with a U2000 spectrophotometer (Shimazu, Japan). PCR amplification was completed with an MJ Mini thermal cycler (Bio-Rad, CA, USA) and subsequent electrophoretic analysis was performed with a BG subMIDI electrophoresis tank (Baygene Biotech Company Limited, Beijing, China) and a ChemiDoc™ XRS+ Imaging System (Bio-Rad, CA, USA).

2.2. Preparation of the C_{60} nanoparticles

C_{60} nanoparticles (nano-C_{60}) was synthesized with a typical solvent-exchange method [37]. Briefly, C_{60} toluene dispersion (1 mg mL^{-1}) was mixed with equal volume of distilled water and stood at room temperature for 5 min. The mixture was subjected to continuous ultrasonic treatment for about 14 h until C_{60} completely transferred from toluene phase into aqueous phase, resulting in a brown nano-C_{60} dispersion.

2.3. Preparation of the signal probe labeled Au-nano-C_{60}/NGS signal tags

The nanohybrid of C_{60} nanoparticles decorated nitrogen-doped graphene sheet (nano-C_{60}/NGS) was synthesized via a simple non-covalent method. Firstly, Nitrogen-doped graphene sheet (NGS) was added into distilled water and pH was adjusted to 10 using 0.5 M NaOH, and the mixture was treated with ultrasound to obtain a homogeneous solution, after which the prepared nano-C_{60} was added into the NGS solution and stirred continuously for 12 h. The product was centrifuged and washed with distilled water three times and re-dispersed into an aqueous solution to a final concentration of 1 mg mL^{-1}.

With sodium borohydride ($NaBH_4$) treatment, gold nanoparticles (AuNPs) were bound to the surface of nano-C_{60}/NGS via strong Au-nitrogen bonds. Briefly, the mixture of 100 μL of

$HAuCl_4$ (1 wt%) and 1 mL of nano-C_{60}/NGS was stirred for 15 min, and $NaBH_4$ solution (4 mg mL^{-1}) was slowly added in drips and stirred for 30 min, and the product was collected after centrifugation at 8000 rpm and washing with distilled water three times and was re-dispersed in distilled water. For tracer label preparation, the AuNPs decorated nano-C_{60}/NGS (Au-nano-C_{60}/NGS) was mixed with thiol-modified signal probes (2 μM) with continuous stirring at 4 ºC overnight.

2.4. Fabrication of the proposed biosensor

Firstly, the bare GCE was cleaned with alumina powder (0.3 and 0.05 μm) and rinsed in turn with ultra-pure water and ethanol to prepare a smooth surface, followed by electrodeposition with $HAuCl_4$ (1 wt%) for 30 s to obtain a uniformly spread AuNPs film. The AuNPs-modified electrode was then immersed with 10 μL of avidin (100 μg mL^{-1}) for 14 h at 4 ºC, incubated with 20 μL of biotin-modified capture probes (2 μM) for 1 h at 4 ºC, and then treated with 6 μL of BSA (0.25 wt%) for 30 min to block nonspecific binding sites. Subsequently, various concentrations of the target DNA was incubated on the electrode surface at 37 ºC for 2 h, hybridized for 2 h with 15 μL of tracer labels at 37 ºC, and then incubated with TOAB to induce the inherent electroactivity of the signal tag (Au-nano-C_{60}/NGS). The unbound substances of each step were removed from the electrode with distilled water. The typical sandwich hybridization and subsequent incubation with TOAB resulted in a well-defined peak current for sensitive electrochemical detection of MTB IS6110 sequence.

2.5. Clinical sample treatment

Sputum specimens of TB patients were collected in the early morning, liquefied with 1 M

NaOH and centrifuged, and the precipitate was resuspended in distilled water and stored at -80 ºC.

2.6. DNA extraction and PCR amplification

The genome DNA of MTB, *S. aureus*, *C. albicans* and clinical samples was extracted using a commercial kit (TIANGEN, Beijing, China), and a 129 bp fragment within IS6110, a 90 bp sequence within Nuc and a 654 bp sequence within the *C. albicans* 18S ribosomal DNA (18S rDNA) were amplified with Premix Taq™ (TaKaRa, Dalian, China). The procedures of PCR amplification were depicted in Table 3. Additionally, the denatured PCR products were prepared for electrochemical analysis with the following procedures: the obtained PCR product was heated at 100 ºC for 7 min to obtain single-stranded DNA and immediately placed on ice for 5 min to avoid renaturation of the DNA as described in previously reported work [38].

3. Results and discussions

3.1. Characterizations of the as-prepared nanocomposite

Field emission scanning electron microscope (FE-SEM) was employed to characterize the structural features of the as-prepared signal tags (Au-nano-C_{60}/NGS). NGS presented a typical lamellate structure with crest-like protuberance (Fig. 2A), and doping nano-C_{60} resulted in abundant nanospheres on the surface of NGS (Fig. 2B). Fig. 2C presents the bright spots of AuNPs on the surface of nano-C_{60}/NGS after AuNPs bonded with nitrogen groups, indicating successful synthesis of Au-nano-C_{60}/NGS. In addition, UV-vis was carried out to investigate the interfacial features of such nanocomposite, as shown in Fig. 2D. In contrast to the absorption band of nano-C_{60}/NGS, Au-nano-C_{60}/NGS showed an extra absorption peak at

520 nm, which is specific of AuNPs [39], further confirming the results from FE-SEM.

3.2. Sensing mechanism of the proposed biosensor

The role of TOAB was studied to investigate the mechanism of the proposed biosensor by recording the DPV response of differently modified electrodes in phosphate buffer (0.1 M, pH 7.0). Fig. 3A shows the DPV measurement of the proposed biosensor with 10 nM target DNA incubated respectively with (1) SPs labeled Au-nano-C_{60}/NGS, without TOAB treatment (curve a); (2) TOAB, without incubation of SPs labeled Au-nano-C_{60}/NGS (curve b); (3) SPs labeled Au-nano-C_{60}/NGS and TOAB (curve c). A distinct peak current at -0.1 V is present in curve c but absent in curve a or b. The result was consistent with previous report that TOAB could arouse the inherent electroactivity of C_{60} [11,12]. Additionally, DPV response of SPs labeled Au-nano-C_{60}/NGS and SPs labeled Au-nano-C_{60} (curve c and d) was examined to evaluate the specific effect of nano-C_{60}/NGS for signal amplification, and curve d showed a poor peak current compared with curve a, indicating that the use of Au-nano-C_{60}/NGS nanohybrid as a signal tag enhances the sensitivity of the electrochemical biosensor, probably because: (1) NGS with its large surface served as a suitable matrix to bear a large amount of nano-C_{60}, as shown in Fig. 2B and Fig. 2C; (2) the introduction of conductive NGS facilitated electron transfer; (3) compared with nano-C_{60}/NGS, sole nano-C_{60} lacks chemical modification for metal nanoparticles anchoring [38], leading to inferior conductivity. This was confirmed with FE-SEM scan images (Fig. 3B) where nano-C_{60} and AuNPs were mostly separated except for a few clusters bounded via physical adsorption. Additionally, the nano-C_{60}/NGS nanocomposite is endowed with the distinctive conductivity of NGS, which is absent in other functionalized nano-C_{60} composites like BSA-modified C_{60} [38], in which the

non-conductivity property of the protein hindered electron transfer. The introduction of the support matrix of NGS, with multiple active sites for AuNPs, incorporates nano-C_{60}, forming a stable and efficient structure, which not only promoted electron transfer due to the highly conductivity of AuNPs and NGS, but also provided a favorable microenvironment for target recognition via the strong Au-S bond.

3.3. Optimization of experimental conditions

In order to obtain optimal performance of the biosensor, optimization of experimental conditions was necessary. Incubation time of avidin, incubation time of CPs, hybridization time of CPs and the target DNA, pH of the phosphate buffer for DPV measurement as well as concentration of TOAB were optimized in this experiment. Experimental conditions were examined in 5 mM $K_3Fe(CN)_6/K_4Fe(CN)_6$ (1:1) solution with 0.1 M KCl with CV measurement ranging from -0.2 V to 0.6 V at a scan rate of 100 mV s^{-1}.

The amount of avidin captured onto the electrode surface and hence the incubation time of avidin directly affects its affinity to biotin-modified CPs. As shown in Fig. 4A, increase in CV signal response did not occur until 14 h of incubation, which was used throughout the experiment.

As for the incubation time of CPs, current response increased in the range of 5-60 min and started to decline at 90 min (Fig. 4B), so the incubation time of CPs was selected as 60 min.

The hybridization efficiency between CPs and target would affect sensitivity of the biosensor [40]. Changes of current response with different hybridization time was recorded. As shown in Fig. 4C, the changes in peak current reached maximum with 120 min of

hybridization, so 120 min was selected as the ideal hybridization time in this experiment.

DPV current response increased with the pH of the phosphate buffer in the range of 5 to 7, and declined when pH increased further (Fig. 4D), so DPV measurement was performed in phosphate buffer with a pH of 7 in the study.

TOAB is also an element to possibly affect the DPV signal response. As shown in Fig 4E, current response reached the peak with a TOAB concentration of 10 mM, so the concentration of TOAB was set at 10 mM.

3.4. Electrochemical characterization of the proposed DNA biosensor

EIS was performed to monitor the modification steps of the proposed electrochemical DNA biosensor in 5 mM $K_3Fe(CN)_6/K_4Fe(CN)_6$ (1:1) solution containing 0.1 M KCl and the changes in electron transfer resistance (R_{et}, presented as diameter of the semicircle) was shown in Fig. 5A. AuNPs-modified electrode (curve b) exhibited a significantly lower R_{et} compared to bare GCE (curve a) due to the high conductivity of metal nanoparticles. When avidin self-assembled onto the electrode surface, a large semicircle domain appeared (curve c). Incubation with biotin-modified CPs led to a sharp increase in R_{et} (curve d), indicating abundant CPs was captured onto the modified electrode surface via avidin-biotin affinity. Then the non-conductive BSA (0.25 wt%) was used to block the non-specific sites (curve e). Lastly, the target DNA (10 nM) bound with CPs with half the sequence, resulting in a further increase of R_{et} (curve f).

In addition, CV ranging from -0.2 to 0.6 V in 5 mM $K_3Fe(CN)_6/K_4Fe(CN)_6$ (1:1) solution containing 0.1 M KCl was used to confirm the EIS results. Bare GCE showed a much lower current response than AuNPs modified electrode surface (Fig. 5B). Decreased current

response in curve c demonstrated self-assembly of avidin onto the modified electrode surface. When biotin-CPs was conjugated with avidin, a further decrease in current response was observed. After incubation with BSA (0.25 wt%) and the target DNA (10 nM), the corresponding CV response decreased successively. To sum up, the consistent changes in CV and EIS signal response demonstrated the assembly of the proposed electrochemical DNA biosensor was successful.

3.5. Analytical performance towards IS6110 fragment

DPV was employed to investigate the analytical performance of the proposed biosensor towards IS6110 fragment in 0.1 M phosphate buffer (pH 7.0) with TOAB treatment. As shown in Fig. 6, the DPV signal response presented a neat linear correlation with the logarithm of the target DNA concentration (from 10 fM to 10 nM). The regression equation was $I = 0.642 \lg c + 7.093$ ($R^2 = 0.9966$).

3.6. Anti-interference, reproducibility and stability studies

Specificity of the biosensor is evaluated using DNA fragments similar to the target sequence and gene fragments of common pathogenic agents other than *Mycobacterium tuberculosis* to rule out unintended reaction with non-target DNA fragments. Similar sequences to the target DNA included non-complementary DNA (N-DNA) and single-base-mismatched DNA (S-DNA), the corresponding DPV signal responses shown in Fig. 7A, both producing merely negligible current changes compared with blank control. Fragments of nuc gene from *Staphylococcus aureus* and of the 18S rDNA from *Candida albicans* and corresponding denatured PCR products were subjected to the proposed electrochemical DNA biosensor as pathogenic agent sequences, resulting in insignificant

signal response compared with the target DNA. Comparatively, the current response of denatured IS6110 PCR products from the H37Rv standard strain, although lower than that of the target, was significantly higher than the denatured PCR product of nuc gene and 18S rDNA, demonstrating excellent specificity of the electrochemical DNA biosensor, which is promising in TB clinical identification.

In order to investigate the reproducibility of the proposed electrochemical DNA biosensor, the current response of five different electrodes was recorded with DPV measurement (Fig. 7B), resulting in similar peak current with an RSD of 4.56 %, indicating outstanding reproducibility. As for the stability of the proposed biosensor, successive CV signal response (Fig. 7C) revealed a 2.1 % decrease after 30 cycles of CV scanning, demonstrating the designed signal tags could effectively improve the stability of the biosensor, and the current response of the proposed biosensor, after 21 days at 4 ºC, remains 88.6% of the initial reading (Fig. 7D), indicating acceptable long-term stability.

3.7. The analysis performance for PCR product of clinical samples

In order to evaluate the potential of the proposed DNA biosensor in clinical application, similar to previously reported works [35], denatured PCR products (of clinical sputum samples from 7 non-tuberculosis patients and 17 tuberculosis patient) were analyzed by the proposed electrochemical test. As shown in Fig. 8, DPV response of the denatured PCR products from the non-tuberculosis group ($\overline{X}$ = 2.79 ± 0.48 μA, n=7) was much lower than that from the TB group ($\overline{X}$ = 5.21 ± 0.54 μA, n=17). These results were consistent with that from PCR (bright bands representing positive TB cases), and therefore the proposed biosensor may hold great potential clinical TB diagnosis.

4. Conclusions

In summary, the nanohybrid of Au-nano-C_{60}/NGS has been successfully synthesized and its application in electrochemical DNA detection investigated. The Au-nano-C_{60}/NGS nanohybrid exhibited high specific surface area, high conductivity, excellent redox activity due to the distinctive synergistic effect of nano-$C_{60,}$ NGS and AuNPs and served as a new signal tag for signal amplification for the first time. Moreover, since such nanohybrid was used directly to generate and enhance signal response, the steps for preparing the biosensor was simplified and leakage of redox molecules was efficiently reduced. Moreover, the biotin-avidin system in the biosensor construction led to significantly increased immobilization of CPs and target analyte recognition, and therefore enhanced detection sensitivity. With these merits, the proposed electrochemical DNA biosensor is able to detect IS6110 fragments at fmol level with excellent specificity, reproducibility and stability and thus may be of great use in clinical practice.

Acknowledgements

This work is supported by the National Science and Technology Major Project (2018ZX10302302003), National Natural Science Foundation of China (81601856, 81570010), the Third Batch of Young Backbone Teachers Funding Program in Colleges and Universities of Chongqing City (2016 No. 53) and Funds for Young Science and Technology Talent Cultivation Plan of Chongqing City (cstc2014kjrc-qnrc00004).

References

[1] World Health Organization. (2018). Global tuberculosis report 2018. World Health Organization. http://www.who.int/iris/handle/10665/274453.

[2] B. Mathema, N.E. Kurepina, P.J. Bifani, B.N. Kreiswirth, Molecular Epidemiology of Tuberculosis: Current Insights, Clin. Microbiol. Rev. 19 (2006) 658.

[3] D. Thierry, M.D. Cave, K.D. Eisenach, J.T. Crawford, J.H. Bates, B. Gicquel, J.L. Guesdon, IS6110, an IS-like element of Mycobacterium tuberculosis complex, Nucleic Acids Res. 18 (1990) 188-188.

[4] M.D. Cave, K.D. Eisenach, G. Templeton, M. Salfinger, G. Mazurek, J.H. Bates, J.T. Crawford, Stability of DNA fingerprint pattern produced with IS6110 in strains of *Mycobacterium tuberculosis*, J. Clin. Microbiol. 32 (1994) 262.

[5] L. Rotariu, F. Lagarde, N. Jaffrezic-Renault, C. Bala, Electrochemical biosensors for fast detection of food contaminants – trends and perspective, TrAC Trends in Analytical Chemistry. 79 (2016) 80-87.

[6] K. Vikrant, N. Bhardwaj, S.K. Bhardwaj, K.-H. Kim, A. Deep, Nanomaterials as efficient platforms for sensing DNA, Biomaterials 214 (2019) 119215.

[7] C. Yang, M.E. Denno, P. Pyakurel, B.J. Venton, Recent trends in carbon nanomaterial-based electrochemical sensors for biomolecules: A review, Anal. Chim. Acta 887 (2015) 17-37.

[8] Y. Chen, X. Liu, S. Guo, J. Cao, J. Zhou, J. Zuo, L. Bai, A sandwich-type electrochemical aptasensor for Mycobacterium tuberculosis MPT64 antigen detection using C60NPs decorated N-CNTs/GO nanocomposite coupled with conductive PEI-functionalized

metal-organic framework, Biomaterials 216 (2019) 119253.

[9] L. Bai, Y. Chen, Y. Bai, Y. Chen, J. Zhou, A. Huang, Fullerene-doped polyaniline as new redox nanoprobe and catalyst in electrochemical aptasensor for ultrasensitive detection of *Mycobacterium tuberculosis* MPT64 antigen in human serum, Biomaterials 133 (2017) 11-19.

[10] G. Lai, F. Yan, H. Ju, Dual Signal Amplification of Glucose Oxidase-Functionalized Nanocomposites as a Trace Label for Ultrasensitive Simultaneous Multiplexed Electrochemical Detection of Tumor Markers, Anal. Chem. 81 (2009) 9730-9736.

[11] J. Han, Y. Zhuo, Y.-Q. Chai, Y. Xiang, R. Yuan, New Type of Redox Nanoprobe: C60-Based Nanomaterial and Its Application in Electrochemical Immunoassay for Doping Detection, Anal. Chem. 87 (2015) 1669-1675.

[12] C. Ye, X. Zhong, R. Yuan, Y. Chai, A novel ECL biosensor based on C60 embedded in tetraoctylammonium bromide for the determination of glucose, Sens. Actuators, B 199 (2014) 101-107.

[13] Z. Wang, Z. Dai, Carbon nanomaterial-based electrochemical biosensors: an overview, Nanoscale 7 (2015) 6420-6431.

[14] C. Ye, X. Zhong, Y. Chai, R. Yuan, Sensing glucose based on its affinity for concanavalin A on a glassy carbon electrode modified with a C_{60} fullerene nanocomposite, Microchim. Acta 182 (2015) 2215-2221.

[15] Q. Zhou, H. Xue, Y. Zhang, Y. Lv, H. Li, S. Liu, Y. Shen, Y. Zhang, Metal-Free All-Carbon Nanohybrid for Ultrasensitive Photoelectrochemical Immunosensing of alpha-Fetoprotein, ACS Sens. 3 (2018) 1385-1391.

[16] S. Afreen, K. Muthoosamy, S. Manickam, U. Hashim, Functionalized fullerene (C_{60}) as a potential nanomediator in the fabrication of highly sensitive biosensors, Biosens. Bioelectron. 63 (2015) 354-364.

[17] P.K. Brahman, L. Suresh, V. Lokesh, S. Nizamuddin, Fabrication of highly sensitive and selective nanocomposite film based on CuNPs/fullerene-C_{60}/MWCNTs: An electrochemical nanosensor for trace recognition of paracetamol, Anal. Chim. Acta 917 (2016) 107-116.

[18] P.K. Brahman, N. Pandey, S.N. Topkaya, R. Singhai, Fullerene–C_{60}–MWCNT composite film based ultrasensitive electrochemical sensing platform for the trace analysis of pyruvic acid in biological fluids, Talanta 134 (2015) 554-559.

[19] J.W. Lee, J.M. Ko, J.-D. Kim, Hydrothermal preparation of nitrogen-doped graphene sheets via hexamethylenetetramine for application as supercapacitor electrodes, Electrochim. Acta 85 (2012) 459-466.

[20] L. Qu, Y. Liu, J.-B. Baek, L. Dai, Nitrogen-Doped Graphene as Efficient Metal-Free Electrocatalyst for Oxygen Reduction in Fuel Cells, ACS Nano 4 (2010) 1321-1326.

[21] H. Fan, Y. Li, D. Wu, H. Ma, K. Mao, D. Fan, B. Du, H. Li, Q. Wei, Electrochemical bisphenol A sensor based on N-doped graphene sheets, Anal. Chim. Acta 711 (2012) 24-28.

[22] Z. Mou, Y. Wu, J. Sun, P. Yang, Y. Du, C. Lu, TiO_2 Nanoparticles-Functionalized N-Doped Graphene with Superior Interfacial Contact and Enhanced Charge Separation for Photocatalytic Hydrogen Generation, ACS Appl. Mater. Interfaces 6 (2014) 13798-13806.

[23] Z. Li, X. Li, Y. Zong, G. Tan, Y. Sun, Y. Lan, M. He, Z. Ren, X. Zheng, Solvothermal synthesis of nitrogen-doped graphene decorated by superparamagnetic Fe_3O_4 nanoparticles and their applications as enhanced synergistic microwave absorbers, Carbon 115 (2017) 493-502.

[24] K. Chang, D. Geng, X. Li, J. Yang, Y. Tang, M. Cai, R. Li, X. Sun, Ultrathin MoS_2/Nitrogen-Doped Graphene Nanosheets with Highly Reversible Lithium Storage, Adv. Energy Mater. 3 (2013) 839-844.

[25] J. Wu, J. He, C. Zhang, J. Chen, Y. Niu, Q. Yuan, C. Yu, PdPt nanoparticles anchored on the N-G with the integration of PANI nanohybrids as novel redox probe and catalyst for the detection of rs1801177, Biosens. Bioelectron. 102 (2018) 403-410.

[26] M. Chen, C. Hou, D. Huo, J. Bao, H. Fa, C. Shen, An electrochemical DNA biosensor based on nitrogen-doped graphene/Au nanoparticles for human multidrug resistance gene detection, Biosens. Bioelectron. 85 (2016) 684-691.

[27] H. Huang, G. Jie, R. Cui, J.-J. Zhu, DNA aptamer-based detection of lysozyme by an electrochemiluminescence assay coupled to quantum dots, Electrochem. Commun. 11 (2009) 816-818.

[28] J. Chen, C. Yu, Y. Zhao, Y. Niu, L. Zhang, Y. Yu, J. Wu, J. He, A novel non-invasive detection method for the FGFR3 gene mutation in maternal plasma for a fetal achondroplasia diagnosis based on signal amplification by hemin-MOFs/PtNPs, Biosens. Bioelectron. 91 (2017) 892-899.

[29] Y. Yu, C. Yu, Y. Niu, J. Chen, Y. Zhao, Y. Zhang, R. Gao, J. He, Target triggered cleavage effect of DNAzyme: Relying on Pd-Pt alloys functionalized Fe-MOFs for amplified

detection of Pb2+, Biosens. Bioelectron. 101 (2018) 297-303.

[30] C. Zhang, J. Lou, W. Tu, J. Bao, Z. Dai, Ultrasensitive electrochemical biosensing for DNA using quantum dots combined with restriction endonuclease, Analyst 140 (2015) 506-511.

[31] P. Teengam, W. Siangproh, A. Tuantranont, T. Vilaivan, O. Chailapakul, C.S. Henry, Electrochemical impedance-based DNA sensor using pyrrolidinyl peptide nucleic acids for tuberculosis detection, Anal. Chim. Acta 1044 (2018) 102-109.

[32] F. Li, Y. Yu, Q. Li, M. Zhou, H. Cui, A Homogeneous Signal-On Strategy for the Detection of rpoB Genes of *Mycobacterium tuberculosis* Based on Electrochemiluminescent Graphene Oxide and Ferrocene Quenching, Anal. Chem. 86 (2014) 1608-1613.

[33] Y. Chen, Y. Li, Y. Yang, F. Wu, J. Cao, L. Bai, A polyaniline-reduced graphene oxide nanocomposite as a redox nanoprobe in a voltammetric DNA biosensor for *Mycobacterium tuberculosis*, Microchim. Acta 184 (2017) 1801-1808.

[34] A. Cannas, D. Goletti, E. Girardi, T. Chiacchio, L. Calvo, G. Cuzzi, M. Piacentini, H. Melkonyan, S.R. Umansky, F.N. Lauria, G. Ippolito, L.D. Tomei, *Mycobacterium tuberculosis* DNA detection in soluble fraction of urine from pulmonary tuberculosis patients, The International Journal of Tuberculosis and Lung Disease 12 (2008) 146-151.

[35] R.R. McDonald, N.A. Antonishyn, T. Hansen, L.A. Snook, E. Nagle, M.R. Mulvey, P.N. Levett, G.B. Horsman, Development of a Triplex Real-Time PCR Assay for Detection of Panton-Valentine Leukocidin Toxin Genes in Clinical Isolates of Methicillin-Resistant, J. Clin. Microbiol. 43 (2005) 6147-6149.

[36] K. Makimura, S.Y. Murayama, H. Yamaguchi, Detection of a wide range of medically important fungi by the polymerase chain reaction, J. Med. Microbiol. 40 (1994) 358-64.

[37] K. Gai, B. Shi, X. Yan, D. Wang, Effect of Dispersion on Adsorption of Atrazine by Aqueous Suspensions of Fullerenes, Environ. Sci. Technol. 45 (2011) 5959-5965.

[38] L. Wang, E. Hua, M. Liang, C. Ma, Z. Liu, S. Sheng, M. Liu, G. Xie, W. Feng, Graphene sheets, polyaniline and AuNPs based DNA sensor for electrochemical determination of BCR/ABL fusion gene with functional hairpin probe, Biosens. Bioelectron. 51 (2014) 201-207.

[39] Y. Chang, E. Lee, J. Kim, Y.-W. Kwon, Y. Kwon, J. Kim, Efficient in vivo direct conversion of fibroblasts into cardiomyocytes using a nanoparticle-based gene carrier, Biomaterials 192 (2019) 500-509.

[40] J.J. Gooding, Electrochemical DNA Hybridization Biosensors, Electroanalysis 14 (2002) 1149-1156.

Table 1 Comparison with other electrochemical biosensors for the MTB DNA determination.

Analytical methods	Target	Linear range	LOD	Ref.
SWV	mycobacterial DNA	10^{-14} - 10^{-9} M	8.7×10^{-15} M	[30]
EIS	mycobacterial DNA	2 - 200 nM	1.24 nM	[31]
ECL	rpoB gene	0.1 - 100 nM	0.04 nM	[32]
DPV	IS6110	0.1 pM - 10 nM	50 fM	[33]
DPV	IS6110	10 fM - 10 nM	3 fM	Present work

SWV: square wave voltammetric; ECL: electrochemiluminescent.

Table 2 Details of DNA sequences used in this experiment.

Oligonucleotide sequences used in this work (5'-3')	
Target (IS6110)	AGACCTCACCTATGTGTCGA
CPs	GGTGAGGTCTAAAAA-Biotin
SPs	SH-$(CH_2)_6$-AAAAATCGACACATA
Single-base-mismatched DNA	AGACCTCACCTATGTCTCGA
Non-complementary DNA	TTCAGCTCAGGGATGACGTC
Nuc	CTTTAGTTGTAGTTTCAAGT
Nuc-F	CTTTAGTTGTAGTTTCAAGT
Nuc-R	CATCGTGGAAGCGACCCGCCAG
18S rDNA	CGTCGTAGTCTTAACCATAA
18S rDNA-F	ACTTTCGATGGTAGGATAG
18S rDNA-R	TGATCGTCTTCGATCCCCTA
IS6110-F	ACCAGCACCTAACCGGCTGTGG
IS6110-R	CATCGTGGAAGCGACCCGCCAG

Nuc: staphylococcal nuclease gene; 18S rDNA:18S ribosomal DNA; F: forward primer; R: reverse primer.

Table 3 Procedures for PCR amplification of IS6110 fragment, nuc gene and 18S rDNA.

Gene name	Initial denaturation	Denaturation	Annealing	Extention	Cycles	Final extention
IS6110	94 ºC 5 min	94 ºC 30 s	62 ºC 30 s	72 ºC 1 min	20	72 ºC 5 min
Nuc	95 ºC 10 min	95 ºC 15 s	58 ºC 30 s	70 ºC 30 s	40	70 ºC 2 min
18S rDNA	94 ºC 3 min	94 ºC 30 s	50 ºC 30 s	68 ºC 45 s	35	68 ºC 7 min

Figure captions:

Fig. 1. Stepwise process of the fabrication of the proposed electrochemical biosensor.

Fig. 2. FE-SEM scan images of (A) NGS, (B) nano-C_{60}/NGS and (C) Au-nano-C_{60}/NGS. (D) UV-vis absorption spectra of (a) nano-C_{60}/NGS and (b) Au-nano-C_{60}/NGS.

Fig. 3. (A) DPV response of differently modified electrodes in phosphate buffer (0.1 M, pH 7.0): the proposed biosensor with target DNA (10 nM) incubated respectively with (a) SPs labeled Au-nano-C_{60}/NGS, without TOAB treatment; (b) TOAB, without incubation of SPs labeled Au-nano-C_{60}/NGS; (c) SPs labeled Au-nano-C_{60}/NGS and TOAB; and (d) SPs labeled Au-nano-C_{60} and TOAB; (B) FE-SEM of Au-nano-C_{60}. Error bars represented the standard deviation (n=3).

Fig. 4. Effect of (A) the incubation time of avidin; (B) the incubation time of CPs; (C) the hybridization time between CPs and target DNA; (E) pH of phosphate buffer; and (F) TOAB concentration. Error bars represented the standard deviation (n=3).

Fig. 5. EIS (A) and CV (B) of (a) bare GCE, (b) AuNPs modified GCE, (c) avidin/AuNPs modified GCE, (d) CPs/avidin/AuNPs modified GCE, (e) BSA/CPs/avidin/AuNPs modified GCE, and (f) BSA/CPs/avidin/AuNPs modified GCE with target DNA (10 nM). Error bars represented the standard deviation (n=3).

Fig. 6. The DPV current response of various concentrations of IS6110 fragments, and the calibration plot obtained by regressing DPV current responses on the logarithm of various IS6110 fragment concentration is presented in the inset. Error bars represented the standard deviation (n=3).

Fig. 7. (A) Interference studies. The inset showed agarose electrophoresis imaging of IS6110

fragment, nuc gene and 18S rDNA. Error bars represented the standard deviation (n=3). (B) Reproducibility of the proposed electrochemical biosensor (n = 5) incubated with 1 nM target DNA. (C) Stability of the proposed electrochemical biosensor for continuous CV scanning (30 cycles). (D) Long-term stability of the proposed biosensor incubated with 1 nM target DNA.

Fig. 8. PCR products of clinical sputum samples analyzed by the proposed electrochemical assay (the red bars represented non-tuberculosis patients and the yellow ones represented tuberculosis patients) and agarose electrophoresis imaging (the inset). Error bars represented the standard deviation (n=3).

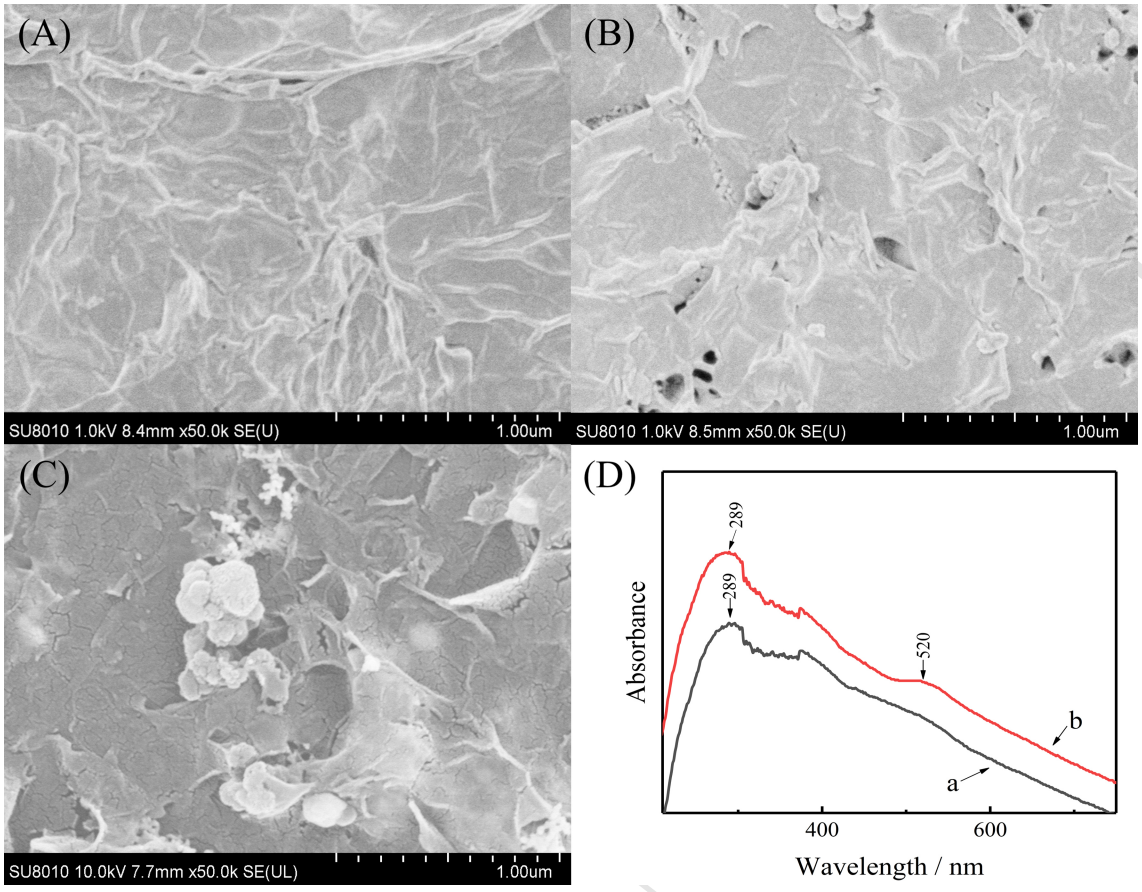

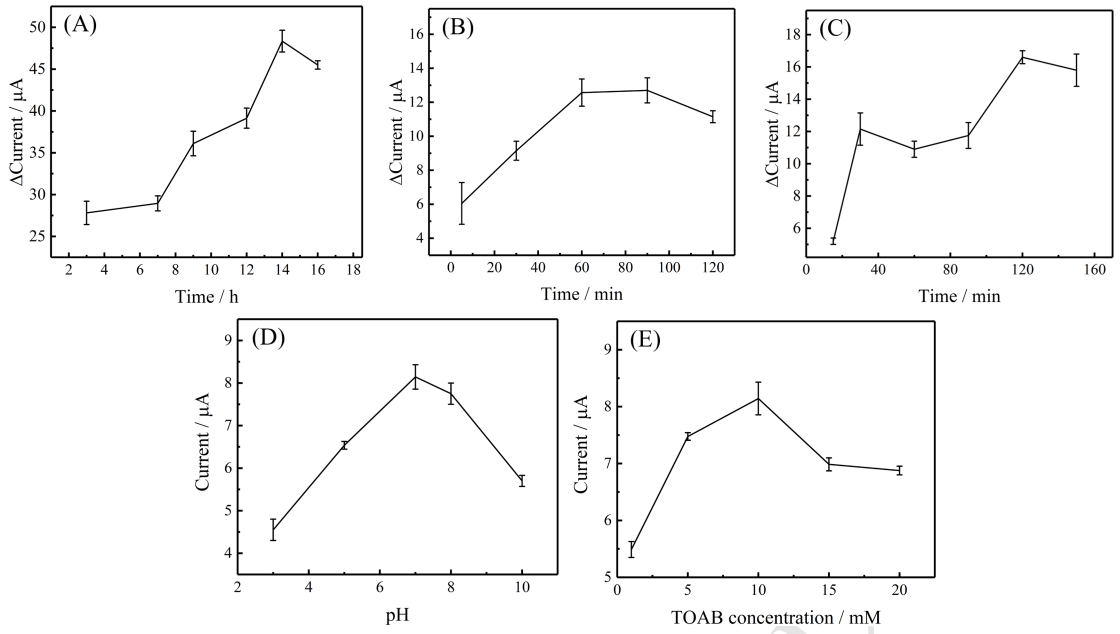

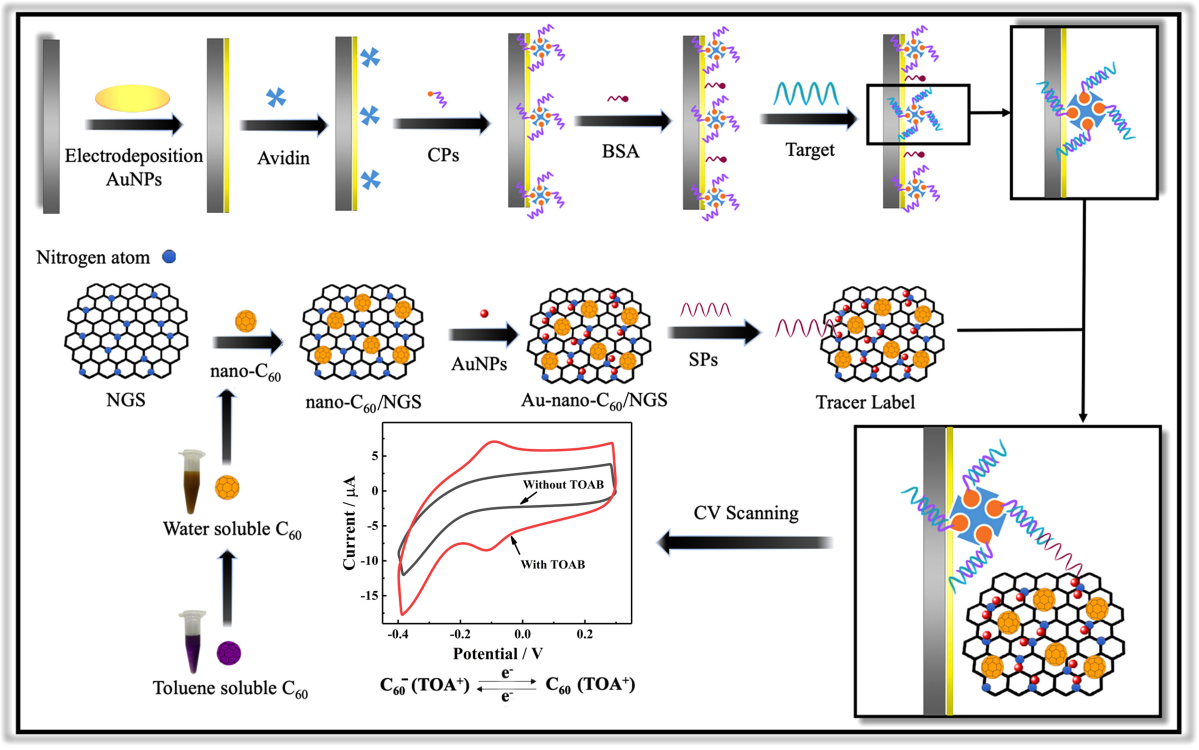

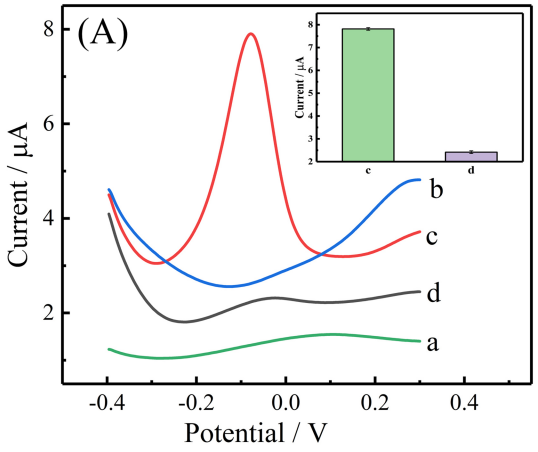

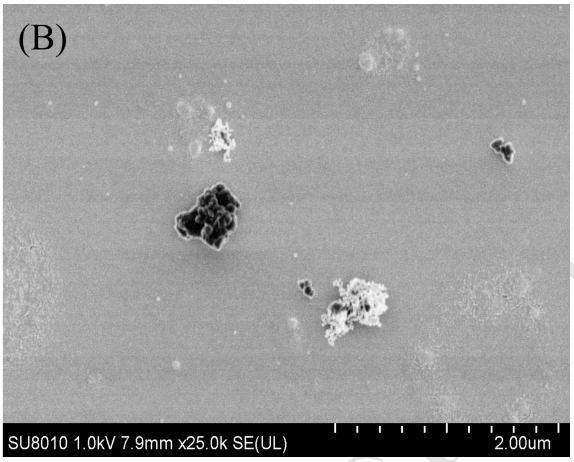

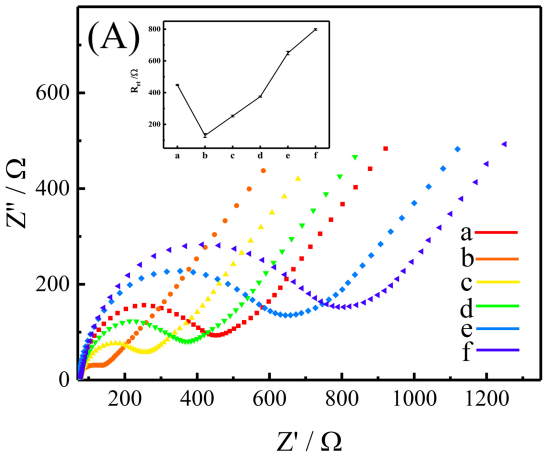

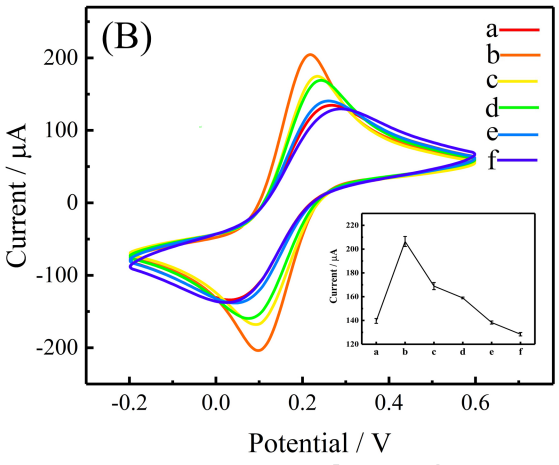

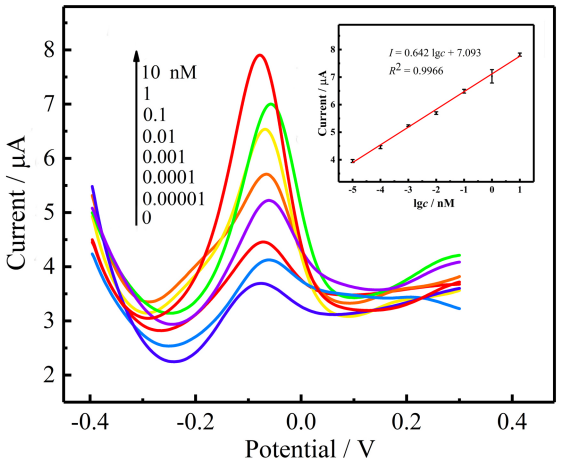

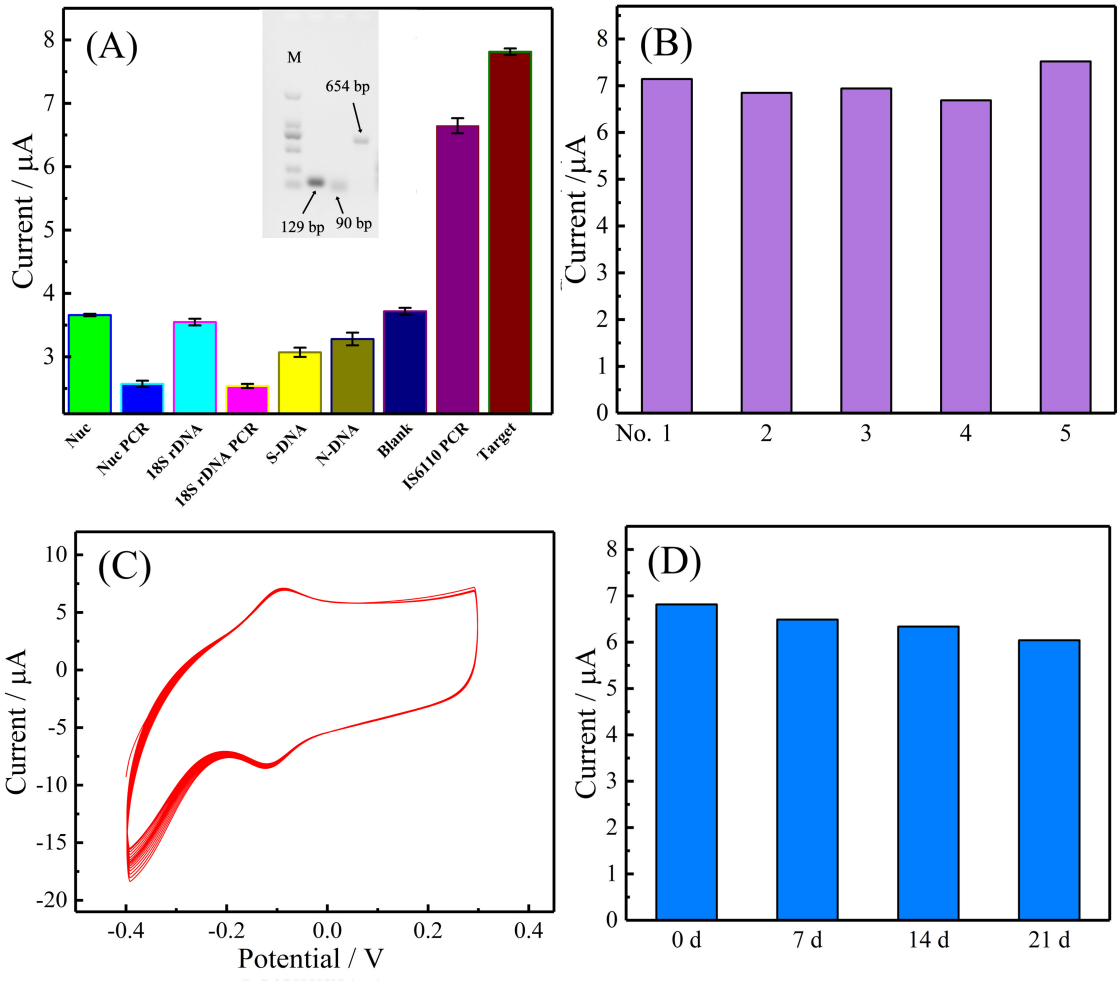

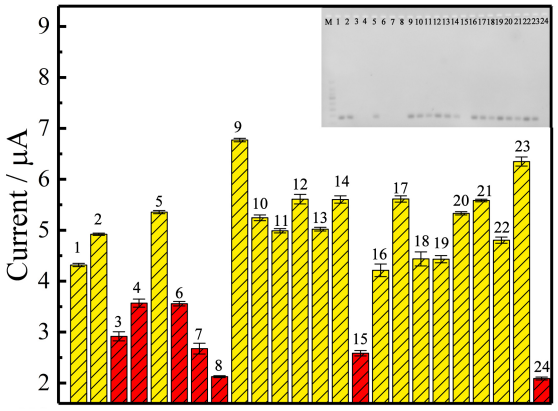

Highlights

- Gold nanoparticles decorated fullerene nanoparticles/nitrogen-doped graphene nanosheet (Au-nano-C_{60}/NGS) without additional redox molecules was directly employed as a signal tag in MTB DNA detection for the first time.
- Nitrogen-doped graphene nanosheet combined with fullerene nanoparticles and gold nanoparticles resulted in high conductivity and outstanding redox activity.
- Preliminary application of the proposed biosensor in clinical detection displayed satisfying results.

Declaration of interests

☒ The authors declare that they have no known competing financial interests or personal relationships that could have appeared to influence the work reported in this paper.

☐The authors declare the following financial interests/personal relationships which may be considered as potential competing interests:

Conflict of Interest

The authors declare that there are no conflicts of interest.